DOI: 10.1002/ejic.201001030

A Conspicuous Deprotonation in Complexes of Diphenyllead(IV) with Ligands Containing Both Semicarbazone and Thiosemicarbazone Chains

José S. Casas,*[a] Estefanía Castro-Vidal,[a] María S. García-Tasende,*[a] Agustín Sánchez,[a] José Sordo,[a] Ángeles Touceda,[a] and Ezequiel M. Vázquez-López[b]

Keywords: Lead / Diphenyllead(IV) / O ligands / S ligands / Partial deprotonation

In the search for new chelating agents for organolead(IV) ions, 2,6-diacetylpyridine was sequentially condensed with semicarbazide and 4-methylthiosemicarbazide to give H_2L^1. According to an X-ray study, this molecule is nearly planar with the semicarbazone (SC) and the thiosemicarbazone (TSC) chains in "open-arm" and "closed-arm" orientations, respectively. Similar condensation of 2,3-butanedione with semicarbazide and 4-methylthiosemicarbazide or with 4-phenylsemicarbazide and 4-phenylthiosemicarbazide afforded H_2L^2 and H_2L^3, respectively. The reactions of H_2L^x with diphenyllead(IV) diacetate in methanol gave the complexes $[PbPh_2(HL^1)](OAc)_{0.75}Cl_{0.25}\cdot 2.375H_2O$, $[PbPh_2(OAc)(HL^2)]\cdot MeOH$ and $[PbPh_2(H_{0.5}L^3)(MeOH)](OAc)_{0.5}$. When the latter was recrystallised from dmso, the new derivative $[PbPh_2(L^3)(dmso)]\cdot 2dmso$ was isolated. The X-ray study of the H_2L^1 complex showed that the ligand, with the TSC chain deprotonated and the SC chain not deprotonated, binds the organometallic moiety through the N3, N4, N5, O1 and S atoms to afford a previously unknown $[PbC_2N_3OS]$ kernel. In the H_2L^2 and H_2L^3 complexes the coordination for the diphenyllead(IV) moiety is the same, with the ligand N,N,S,O-bound, but these complexes differ in the protonation status of the SC chain. In $[PbPh_2(OAc)(HL^2)]\cdot MeOH$ the chain is not deprotonated, and in $[PbPh_2(L^3)(dmso)]\cdot 2dmso$ it is deprotonated. Conspicuously, in $[PbPh_2(H_{0.5}L^3)(MeOH)](OAc)_{0.5}$ the SC "arm" is formally only "half" deprotonated according to the X-ray study and analysis of the occupation factors in the lattice. From a more "chemical" point of view, this complex can be depicted as containing both $(HL^3)^-$ and $(L^3)^{2-}$ ligands in a 1:1 ratio. This partial deprotonation of the SC chain is supported both by a bond length analysis and by ^1H NMR spectroscopy.

Introduction

Lead is one of the seven metals of antiquity and has played a very important role in the progress of mankind. It also, however, constitutes one of the oldest known toxicants for living beings. In humans, lead at blood concentrations $\geq$30 μg/dL affects all major body systems but is particularly damaging for the developing central nervous system of children.[1] Despite the accumulated evidence of the adverse health effects of this metal, lead and its compounds are still widely used, and this makes lead poisoning a recurrent problem in society.[2]

The present approved clinical procedure to deal with lead(II) ("inorganic lead") poisoning is the use of chelating agents that are able to remove the metal from lead-burdened tissue.[3] Theoretically, these agents, once administered, move to the tissue, displace the endogenous ligands to which the metal is bound and form a complex with the metal ion that can be excreted in the urine or faeces. Intravenous calcium sodium edentate (calcium disodium ethylenediaminetetraacetic acid, $CaNa_2$edta) is the most commonly used chelating agent for "inorganic lead" poisoning. This compound binds the Pb^{II} ion through the amino and carboxylic acid groups to form stable chelates[4] but it is mainly distributed extracellularly and appears to cause the redistribution of lead to the brain.[5] An emerging alternative is the water-soluble derivative *meso*-2,3-dimercaptosuccinic acid (dmsa), which has been approved by the US FDA for the treatment of lead intoxication in children.[5] According to a recent review,[6] dmsa in humans is a good chelator for renal lead(II) but occasionally causes significant adverse effects. Thus, even though some chelators are effective for "inorganic lead" poisoning, they all have some drawbacks and are, at present, far from being considered as "ideal" chelating drugs. With respect to organolead(IV) compounds ("organic lead", $PbR_n^{(4-n)+}$), a specific therapy for their toxic effects has yet to be developed.[7]

As part of a programme aimed at preparing new chelators for the treatment of $PbR_n^{(4-n)+}$ poisoning, we describe here the synthesis of some mixed semicarbazone/thiosemicarbazone ligands (H_2L^{1-3}) and their interaction with di-

[a] Departamento de Química Inorgánica, Facultade de Farmacia, Universidade de Santiago de Compostela,
15782 Santiago de Compostela, Galicia, Spain
Fax: +34-981-547102
E-mail: sergio.casas@usc.es
soledad.garcia@usc.es
[b] Departamento de Química Inorgánica, Facultade de Química, Universidade de Vigo,
36310 Vigo, Galicia, Spain
Supporting information for this article is available on the WWW under http://dx.doi.org/10.1002/ejic.201001030.

phenyllead(IV), which was used as a coordination model for the very poisonous dimethyl- and diethyllead(IV) cations. These ligands can bind to the metal ions through the O and S atoms and also through N atoms (Scheme 1). As far as we know, only one mixed ligand similar to H_2L^1 has been used before to prepare a complex – in this case with Sm^{III}.[8]

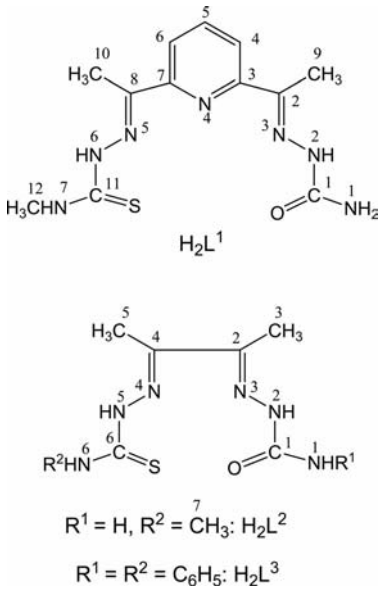

Scheme 1. Semicarbazone/thiosemicarbazone mixed ligands.

Results and Discussion

Synthesis

The semicarbazone/thiosemicarbazone mixed ligands derived from 2,6-diacetylpyridine and 2,3-butanedione diketones were prepared by two consecutive condensation reactions. The first reaction, between the diketone and semicarbazide or 4-phenylsemicarbazide, formed the corresponding semicarbazone (SC^1, SC^2, SC^3); the second reaction, between SC^x and 4-methyl-3-thiosemicarbazide or 4-phenyl-3-thiosemicarbazide, afforded the corresponding mixed ligand H_2L^x (Scheme 1).

Reaction of these ligands with diphenyllead(IV) diacetate gave the complexes $[PbPh_2(HL^1)](OAc)_{0.75}Cl_{0.25}\cdot 2.375H_2O$, $[PbPh_2(OAc)(HL^2)]\cdot MeOH$, $[PbPh_2(H_{0.5}L^3)(MeOH)](OAc)_{0.5}$ and $[PbPh_2(L^3)(dmso)]\cdot 2dmso$. These compounds were studied by X-ray diffraction. The presence of Cl^- in the first complex is plausibly due to the incomplete displacement of this anion from $PbPh_2Cl_2$ during the synthesis of $PbPh_2(OAc)_2$ (see below).

X-ray Studies

Crystal Structure of H_2L^1

The molecular structure of H_2L^1 is shown in Figure 1, and selected structural parameters are listed in Table 1. As far as we know, this is the first ligand of this type to be characterized by X-ray diffraction.

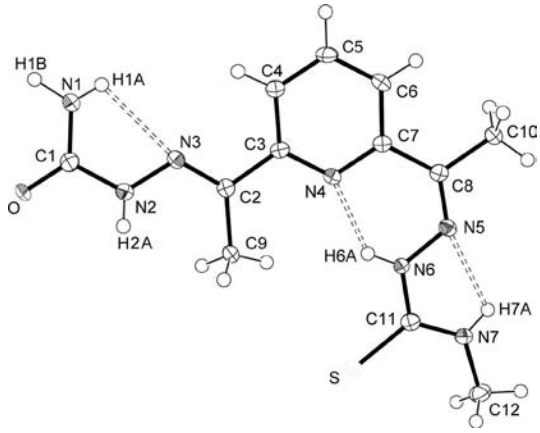

Figure 1. Molecular structure of H_2L^1.

Table 1. Selected bond lengths [Å] and angles [°] for H_2L^1.

S–C(11)	1.692(3)	N(7)–C(11)	1.324(3)
O–C(1)	1.236(3)	N(7)–C(12)	1.453(3)
N(1)–C(1)	1.332(3)	C(2)–C(3)	1.488(3)
N(2)–N(3)	1.365(3)	C(2)–C(9)	1.501(3)
N(2)–C(1)	1.394(3)	C(3)–C(4)	1.396(3)
N(3)–C(2)	1.291(3)	C(4)–C(5)	1.377(4)
N(4)–C(3)	1.345(3)	C(5)–C(6)	1.383(3)
N(4)–C(7)	1.352(3)	C(6)–C(7)	1.395(3)
N(5)–C(8)	1.293(3)	C(7)–C(8)	1.486(3)
N(5)–N(6)	1.368(3)	C(8)–C(10)	1.503(3)
N(6)–C(11)	1.358(3)		
N(3)–N(2)–C(1)	119.6(2)	C(4)–C(3)–C(2)	120.7(2)
C(2)–N(3)–N(2)	117.8(2)	C(5)–C(4)–C(3)	118.9(2)
C(3)–N(4)–C(7)	118.9(2)	C(4)–C(5)–C(6)	119.2(2)
C(8)–N(5)–N(6)	119.4(2)	C(5)–C(6)–C(7)	119.5(2)
C(11)–N(6)–N(5)	119.5(2)	N(4)–C(7)–C(6)	121.3(2)
C(11)–N(7)–C(12)	124.2(2)	N(4)–C(7)–C(8)	118.8(2)
O–C(1)–N(1)	124.7(2)	C(6)–C(7)–C(8)	119.9(2)
O–C(1)–N(2)	118.6(2)	N(5)–C(8)–C(7)	127.9(2)
N(1)–C(1)–N(2)	116.6(2)	N(5)–C(8)–C(10)	114.1(2)
N(3)–C(2)–C(3)	114.4(2)	C(7)–C(8)–C(10)	118.0(2)
N(3)–C(2)–C(9)	124.5(2)	N(7)–C(11)–N(6)	117.1(2)
C(3)–C(2)–C(9)	121.2(2)	N(7)–C(11)–S	124.07(19)
N(4)–C(3)–C(4)	122.1(2)	N(6)–C(11)–S	118.84(18)
N(4)–C(3)–C(2)	117.2(2)		

The values for the bond lengths and angles in the semicarbazone and thiosemicarbazone moieties are in the expected range.[9] The orientation of the SC and TSC chains with respect to the pyridine ring (as "open-arm" and "closed-arm", respectively, Figure 1) is similar to that described for the ligand 2,6-diacetylpyridine bis(thiosemicarbazone) methanol solvate[10] and 2,6-diacetylpyridine bis(*N*-ethyl-thiosemicarbazone).[11] The "closed-arm" orientation of the TSC chain enables the formation of a strong intramolecular hydrogen bond between N(6)–H(6A) and the pyridine nitrogen atom [N(4)] (Figure 1 and Table 2). Apparently, the ligand prefers to "close" the TSC "arm" instead of the SC "arm", suggesting that the partial positive charge on H(6A) is greater than that on H(2A). This situa-

tion is consistent with the easier deprotonation of the TSC chain with respect to the SC chain (see below). Additionally, both chains exhibit the usual intramolecular hydrogen bonds between one hydrogen atom of the amino group and the nitrogen atom of the carbohydrazide group [N(1)–H(1A)···N(3) and N(7)–H(7A)···N(5)], a situation that places N(3) and N(5) *trans* to O and S, respectively. The molecule is nearly planar (*rms* = 0.0970 for all non-hydrogen atoms) and the S and C(10) atoms show the highest deviation from this plane.

Table 2. Hydrogen-bond lengths [Å] and angles [°] in H_2L^1.

D–H···A[a]	*d*(D–H)	*d*(H···A)	*d*(D···A)	<(DHA)
N(1)–H(1A)···N(3)	0.80(3)	2.35(3)	2.665(3)	104(2)
N(6)–H(6A)···N(4)	0.84(3)	1.97(3)	2.642(3)	136(3)
N(7)–H(7A)···N(5)	0.84(3)	2.21(3)	2.635(3)	111(2)
N(1)–H(1A)···O^{i}	0.80(3)	2.22(3)	2.881(3)	140(3)
N(1)–H(1B)···S^{ii}	0.98(3)	2.56(3)	3.531(2)	172(2)
N(2)–H(2A)···S^{iii}	0.79(3)	2.99(3)	3.653(2)	143(3)

[a] Symmetry operators: i = *x* + 1/2, –*y* – 1/2, *z* + 1/2; ii = –*x* – 1/2, *y* – 1/2, –*z* + 1/2; iii = –*x*, –*y*, –*z*.

The N–H protons not involved in the intramolecular hydrogen bonds, along with the O and S atoms, form several intermolecular hydrogen bonds (Table 2) that lead to the arrangement of the molecules in a supramolecular network. One of these interactions, N(1)–H(1A)···O(1)^{i}, the influence of which on the opening of the chain can not be discarded, associates the molecules in chains (Figure S1), whereas adjacent chains are connected by weak N–H···S hydrogen bonds (Figure S2).

Crystal Structure of $[PbPh_2(HL^1)](OAc)_{0.75}Cl_{0.25}\cdot 2.375H_2O$

The molecular structure of $[PbPh_2(HL^1)](OAc)_{0.75}Cl_{0.25}\cdot 2.375H_2O$ is shown in Figure 2 along with the numbering scheme. Selected bond lengths and angles are listed in Table 3. The asymmetric unit consists of the cationic complex $[PbPh_2(HL^1)]^+$, a disordered acetate or chloride anion with occupation factors of 0.75 and 0.25, respectively, and 2.375 molecules of water disordered over four positions with occupation factors of 1 (for O3w), 0.75 (for O1w), 0.25 (for O4w) and 0.375 (for O2w). In the cationic complex the $(HL^1)^-$ ligand has a deprotonated TSC chain and binds the metal atom through the N(3), N(4), N(5), O(1) and S atoms to afford a $[PbC_2N_3OS]$ kernel, which has previously been unknown according to a search of the Cambridge Structural Database.[12] The coordination geometry around the metal atom can be described as a slightly distorted pentagonal bipyramid with the phenyl groups in axial positions and $(HL^1)^-$ on the equatorial plane. The main distortions with regard to the ideal geometry correspond to the C–Pb–C [171.6(2)°] and O–Pb–S [93.77(11)°] bond angles. To achieve their coordination, the TSC and SC chains of the ligand both adopt an (*E*) configuration with respect to the C(2)=N(3) and C(8)=N(5) bonds, and the O and S atoms are *cis* to N(3) and N(5). This arrangement permits the formation of four five-membered chelate rings.

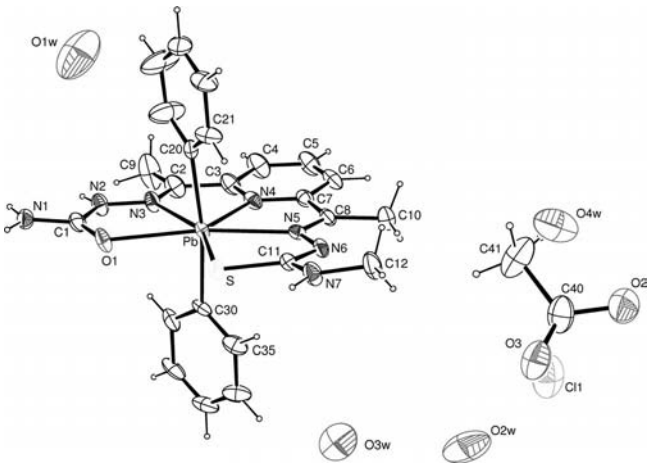

Figure 2. Molecular structure of $[PbPh_2(HL^1)]\cdot(OAc)_{0.75}Cl_{0.25}\cdot 2.375H_2O$.

Table 3. Selected bond lengths [Å] and angles [°] for $[PbPh_2(HL^1)](OAc)_{0.75}Cl_{0.25}\cdot 2.375H_2O$.

Pb–C(20)	2.193(6)	N(5)–N(6)	1.371(7)
Pb–C(30)	2.196(6)	N(6)–C(11)	1.311(9)
Pb–N(5)	2.440(5)	N(7)–C(11)	1.345(9)
Pb–N(4)	2.457(5)	N(7)–C(12)	1.454(9)
Pb–O(1)	2.521(5)	C(2)–C(9)	1.473(11)
Pb–N(3)	2.558(6)	C(2)–C(3)	1.492(10)
Pb–S	2.7226(16)	C(3)–C(4)	1.383(10)
S–C(11)	1.762(7)	C(4)–C(5)	1.389(11)
O(1)–C(1)	1.239(8)	C(5)–C(6)	1.360(11)
N(1)–C(1)	1.342(8)	C(6)–C(7)	1.376(10)
N(2)–C(1)	1.374(9)	C(7)–C(8)	1.464(10)
N(2)–N(3)	1.375(8)	C(8)–C(10)	1.511(9)
N(3)–C(2)	1.296(9)	O(2)–C(40)	1.263(13)
N(4)–C(3)	1.345(9)	O(3)–C(40)	1.184(15)
N(4)–C(7)	1.365(9)	C(40)–C(41)	1.539(17)
N(5)–C(8)	1.295(8)		
C(20)–Pb–C(30)	171.6(2)	N(5)–Pb–S	72.56(13)
N(5)–Pb–N(4)	67.30(18)	O(1)–Pb–S	93.77(11)
N(4)–Pb–N(3)	63.68(18)	O(2)–C(40)–O(3)	125.3(12)
O(1)–Pb–N(3)	62.73(16)		

Deprotonation of the N(6)H group in the TSC chain instead of the N(2)H group in the SC chain is supported by the structural changes experienced by the ligand upon metallation. The TSC moiety partially evolves to the thiol form [*d*(C–S) = 1.692(3) Å in the free ligand and 1.762(7) Å in the complex], and the Pb–N bond lengths suggest stronger interactions with this chain than with the SC chain.

In the crystal, two $[PbPh_2(HL^1)]^+$ cations with the HL^{1-} ligands in the same plane are linked through N(1)–H(1A)···O(1)^{i} hydrogen bonds to form dimers (Figure S3, Table 4). These dimers are in turn connected into chains through N(7)–H(7)···S(1)^{iii} bonds. The packing and the relative location of these chains are shown in Figure S4. A weak π···π

interaction between the pyridine ring and the C(20)–C(25) phenyl ring (centroid–centroid distance 3.927 Å) and a weak C–H···π interaction between the C(23)–H and the C(30)–C(25) phenyl ring (C23–centroid distance 3.465 Å) connect adjacent chains.

Table 4. Hydrogen-bond lengths [Å] and angles [°] in $[PbPh_2(HL^1)](OAc)_{0.75}Cl_{0.25}\cdot 2.375H_2O$.[a]

D–H···A[b]	*d*(D–H)	*d*(H···A)	*d*(D···A)	<(DHA)
N(1)–H(1A)···O(1)^{i}	0.86	2.09	2.902(7)	156.8
N(1)–H(1B)···O(3)^{ii}	0.86	1.98	2.842(10)	176.1
N(1)–H(1B)···Cl^{ii}	0.86	2.39	3.193(12)	156.5
N(2)–H(2)···O(2)^{ii}	0.86	1.95	2.645(10)	136.5
N(2)–H(2)···Cl^{ii}	0.86	2.55	3.317(12)	148.2
N(7)–H(7)···S^{iii}	0.86	2.86	3.502(6)	132.6
N(7)–H(7)···O(3)^{iv}	0.86	2.44	2.974(11)	120.9

[a] Those involving the water molecules are not included. [b] Symmetry operators: i = $-x + 3/2, -y + 1/2, -z + 2$; ii = $x + 1, y, z + 1$; iii = $-x + 1, y, -z + 3/2$; iv = $x + 1/2, -y + 1/2, z + 1/2$.

The acetate and chloride anions interact (Table 4, Figure 3) with the chains without increasing the association. Although the hydrogen atoms of the water molecules were not located, the position of their oxygen atom suggests that they form hydrogen bonds with $[PbPh_2(HL^1)]^+$, AcO^- and Cl^-, giving rise to an extended network.

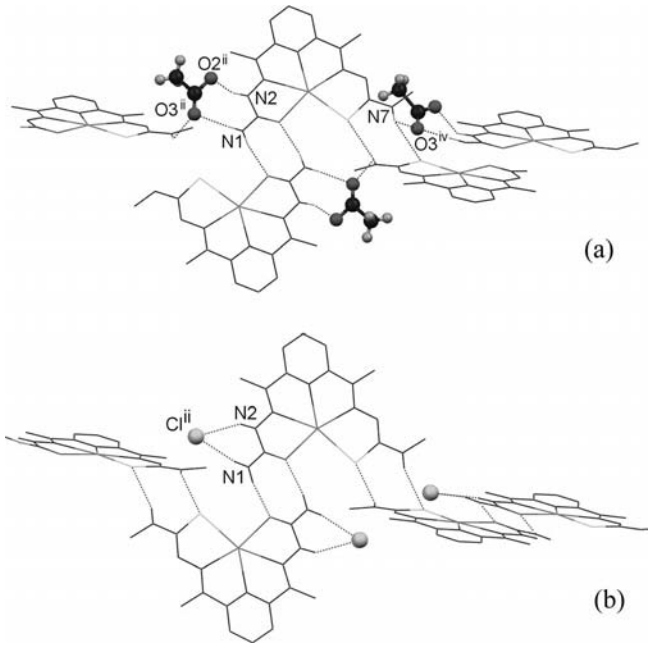

Figure 3. Hydrogen bonds between acetate (a) or chloride (b) anions and the complex cation in $[PbPh_2(HL^1)](OAc)_{0.75}Cl_{0.25}\cdot 2.375H_2O$.

Crystal Structure of $[PbPh_2(OAc)(HL^2)]\cdot MeOH$

The molecular structure and the numbering scheme for this complex are shown in Figure 4, and selected bond lengths and angles are given in Table 5.

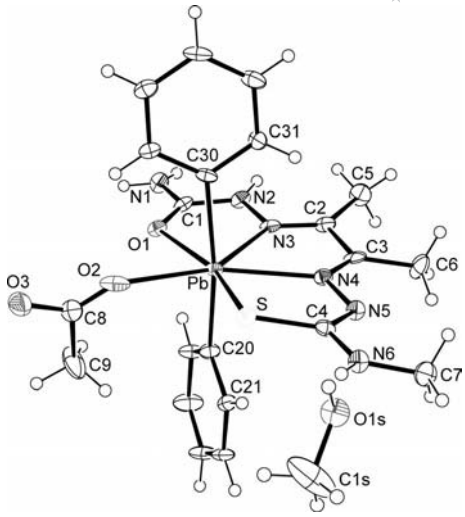

Figure 4. Molecular structure of $[PbPh_2(OAc)(HL^2)]\cdot MeOH$.

Table 5. Selected bond lengths [Å] and angles [°] for $[PbPh_2(OAc)(HL^2)]\cdot MeOH$.

Pb–C(20)	2.182(6)	N(4)–C(3)	1.304(8)
Pb–C(30)	2.183(6)	N(4)–N(5)	1.380(7)
Pb–N(4)	2.467(5)	N(5)–C(4)	1.318(8)
Pb–O(2)	2.496(5)	N(6)–C(4)	1.342(8)
Pb–N(3)	2.579(5)	N(6)–C(7)	1.452(8)
Pb–O(1)	2.603(4)	C(2)–C(3)	1.481(9)
Pb–S	2.7010(17)	C(2)–C(5)	1.512(8)
S–C(4)	1.749(7)	C(3)–C(6)	1.498(9)
O(1)–C(1)	1.239(7)	O(2)–C(8)	1.152(8)
N(1)–C(1)	1.320(8)	O(3)–C(8)	1.260(7)
N(2)–N(3)	1.359(7)	C(8)–C(9)	1.555(10)
N(2)–C(1)	1.378(8)	O(1S)–C(1S)	1.383(10)
N(3)–C(2)	1.295(8)		
C(20)–Pb–C(30)	165.5(2)	S–Pb–N(4)	70.91(13)
O(1)–Pb–O(2)	86.57(15)	N(4)–Pb–N(3)	63.90(18)
O(2)–Pb–S	77.06(12)	N(3)–Pb–O(1)	61.69(16)

The partially deprotonated H_2L^2 ligand coordinates to the organometallic moiety through the S, N(4), N(3) and O atoms to form three five-membered chelate rings, which are almost coplanar (Pb, C1, N2, N3, C2, C3, N4, N5, C4, S; *rms* = 0.1173). The interactions of the metal atom with the TSC "arm" are comparable with those previously discussed for the complex of H_2L^1, but the Pb–O(1) bond with the SC "arm" is slightly weaker in the present derivative. Both the SC and TSC chains adopt an (*E*) configuration to chelate the metal atom, and the C(4)–S bond length in the TSC chain indicates a thione-to-thiol evolution upon deprotonation and metallation. The C=O bond length, however, remains within the range found in free semicarbazones that are not deprotonated.[11]

The reduction in the number of donor atoms in H_2L^2 with respect to H_2L^1 allowed the incorporation of an additional monodentate acetate group on the equatorial plane of the complex (Pb, O1, N3, N4, S, O2; *rms* = 0.0638) and again leads to a distorted pentagonal-bipyramidal arrangement around the metal atom with the phenyl groups in the apical positions. The coordination mode of the acetate differs from that previously observed in some heteroleptic

(monothiosemicarbazone)diphenyllead(IV) complexes[13–15] in which the acetate moiety is anisobidentate and binds to the metal atom with a bite angle of around 50°.

The molecules of the complex associate through intermolecular hydrogen bonds (Table 6) that involve the N(1)H and N(2)H groups from the SC "arm" and the oxygen atoms from the acetate ligand [O(2) and O(3)] to give a chain along the *b* axis (Figure S5). The fact that the N(2)–H group is involved in a hydrogen bond clearly supports the SC chain not being deprotonated. The MeOH molecules, which behave both as hydrogen-bond donors and as double-acceptors, connect the chains and extend the association into a 2D network (Figure S6).

Table 6. Hydrogen-bond lengths [Å] and angles [°] in $[PbPh_2(OAc)(HL^2)]\cdot MeOH$.

D–H···A[a]	*d*(D–H)	*d*(H···A)	*d*(D···A)	<(DHA)
N(1)–H(1A)···O(1S)^{i}	0.86	2.18	3.029(8)	167.8
N(1)–H(1B)···O(2)^{ii}	0.86	2.08	2.935(7)	170.3
O(1S)–H(1S)···S^{iii}	0.82	2.42	3.225(5)	166.4
N(2)–H(2)···O(3)^{ii}	0.86	1.99	2.815(7)	160.6
N(6)–H(6)···O(1S)	0.86	2.08	2.879(7)	154.1

[a] Symmetry operators: i = $x + 1/2, -y + 1/2, z - 1/2$; ii = $-x + 3/2, y - 1/2, -z + 3/2$; iii = $-x + 1, -y + 1, -z + 2$.

Crystal Structures of $[PbPh_2(H_{0.5}L^3)(MeOH)](OAc)_{0.5}$ and $[PbPh_2(L^3)(dmso)]\cdot 2dmso$

The molecular structures of complexes obtained from the H_2L^3 ligand are shown in Figures 5 and 6. Selected bond lengths and angles are listed in Tables 7 and 8.

According to the X-ray study, the reaction of H_2L^3 with diphenyllead(IV) diacetate under conditions similar to those described for H_2L^2 afforded the complex $[PbPh_2(H_{0.5}L^3)(MeOH)](OAc)_{0.5}$, in which the TSC "arm" of H_2L^3 is deprotonated but the SC "arm" is formally only "half" deprotonated. This rather unusual deprotonation behaviour of H_2L^3 was concluded from an analysis of the occupation factors in the lattice. These factors are 1 for all

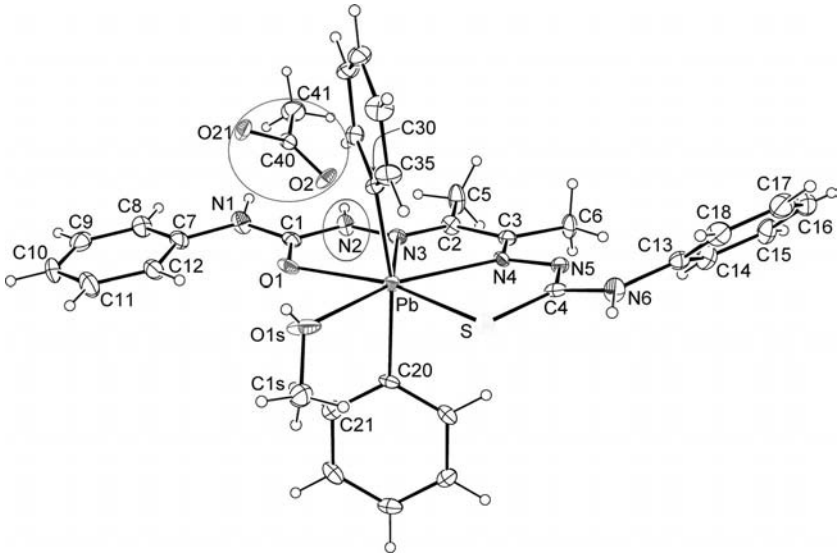

Figure 5. Asymmetric unit of $[PbPh_2(H_{0.5}L^3)(MeOH)](OAc)_{0.5}$. The acetate group and the proton on N2 have occupation factors of 0.5.

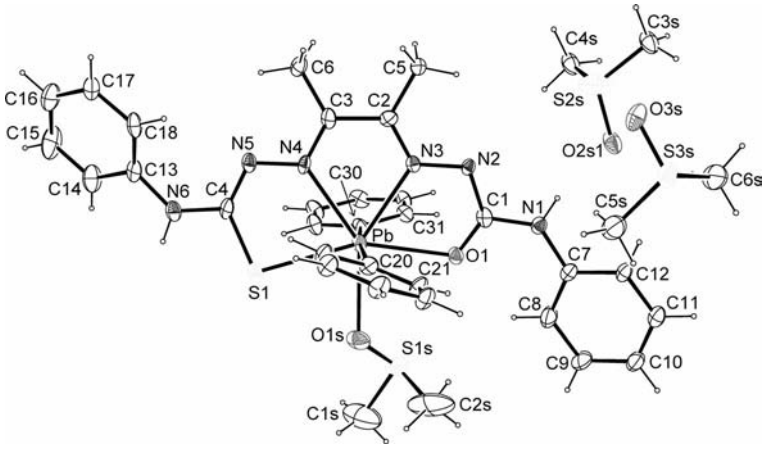

Figure 6. Molecular structure of $[PbPh_2(L^3)(dmso)]\cdot 2dmso$.

Table 7. Selected bond lengths [Å] and angles [°] for $[PbPh_2(H_{0.5}L^3)(MeOH)](OAc)_{0.5}$.

Pb–C(20)	2.175(4)	N(2)–C(1)	1.366 (5)
Pb–C(30)	2.182(4)	N(3)–C(2)	1.300(5)
Pb–N(4)	2.466(3)	N(4)–C(3)	1.305(5)
Pb–N(3)	2.482(3)	N(4)–N(5)	1.380(4)
Pb–O(1)	2.492(3)	N(5)–C(4)	1.311(5)
Pb–O(1S)	2.574(3)	N(6)–C(4)	1.361(5)
Pb–S	2.7475(11)	N(6)–C(13)	1.409(5)
S–C(4)	1.738(4)	C(2)–C(3)	1.461(5)
O(1)–C(1)	1.253(5)	O(1S)–C(1S)	1.408(5)
N(1)–C(1)	1.361(5)	O(2)–C(40)	1.277(9)
N(1)–C(7)	1.407(5)	O(21)–C(40)	1.258(9)
N(2)–N(3)	1.350(5)	C(40)–C(41)	1.603(9)
C(20)–Pb–C(30)	169.21(14)	O(1)–Pb–O(1S)	77.39(11)
N(4)–Pb–N(3)	65.49(11)	N(4)–Pb–S	70.28(8)
N(3)–Pb–O(1)	63.47(10)	O(1S)–Pb–S	83.39(10)

Table 8. Selected bond lengths [Å] and angles [°] for $[PbPh_2(L^3)(dmso)]\cdot 2dmso$.

Pb–C(30)	2.182(10)	C(2)–N(3)	1.300(12)
Pb–C(20)	2.209(10)	C(2)–C(3)	1.484(14)
Pb–N(3)	2.427(7)	C(3)–N(4)	1.310(13)
Pb–N(4)	2.428(8)	C(3)–C(6)	1.479(14)
Pb–O(1)	2.434(6)	N(4)–N(5)	1.383(10)
Pb–O(1s)	2.506(8)	C(4)–N(5)	1.294(13)
Pb–S(1)	2.696(3)	C(4)–N(6)	1.380(13)
S(1)–C(4)	1.755(11)	S(1s)–O(1s)	1.456(9)
O(1)–C(1)	1.277(12)	S(2s)–O(2s2)	1.50(4)
N(1)–C(1)	1.372(13)	S(2s)–O(2s1)	1.505(12)
C(1)–N(2)	1.346(13)	S(3s)–O(3s)	1.493(8)
N(2)–N(3)	1.373(10)		
C(30)–Pb–C(20)	172.9(4)	O(1)–Pb–O(1s)	82.5(2)
N(3)–Pb–N(4)	67.4(2)	N(4)–Pb–S(1)	71.3(2)
N(3)–Pb–O(1)	65.0(2)	O(1s)–Pb–S(1)	73.9(2)

atoms except for the hydrogen atom on N(2) and the acetate atoms, which are 0.5. Although from a crystallographic point of view this compound contains the $(H_{0.5}L^3)^{1.5-}$ ligand, from a more "chemical" point of view it can be depicted as containing both $(HL^3)^-$ and $(L^3)^{2-}$ ligands in a 1:1 ratio.

This partial deprotonation of the SC chain is also supported by ^1H NMR spectroscopy (see below) and by the structural parameters of the complex $[PbPh_2(L^3)(dmso)]\cdot 2dmso$ obtained when $[PbPh_2(H_{0.5}L^3)(MeOH)](OAc)_{0.5}$ was recrystallised from dmso.

In both H_2L^3 complexes, the coordination environment for the diphenyllead(IV) unit is similar to that previously described for $[PbPh_2(OAc)(HL^2)]\cdot MeOH$, with the equatorial plane occupied by the N,N,O,S-tetradentate semicarbazone/thiosemisemicarbazone ligand plus another O-bound (MeOH or dmso) ligand. The $(H_{0.5}L^3)^{1.5-}$ and $(L^3)^{2-}$ ligands have an identical conformation in both complexes, with the O(1) and S atoms *cis* to N(3) and N(4), respectively. As usual, the deprotonated TSC chain evolves from thione (the C=S bond length in free TSCs has an average value of 1.685 Å[9]) to thiol and binds the metal atom through the S and N(4) atoms slightly more strongly in $[PbPh_2(L^3)(dmso)]\cdot 2dmso$ than in $[PbPh_2(H_{0.5}L^3)(MeOH)](OAc)_{0.5}$. More significant are the Pb–O(1) and Pb–N(3) distances, which decrease as deprotonation of the semicarbazone chain increases. Note that the distances in the SC chain (see Tables 7 and 8) also appear to be sensitive to the different degree of H_2L^3 deprotonation [the O(1)–C(1) and N(2)–C(1) bond lengths increase and decrease, respectively, when the degree of deprotonation increases, as one would expect if the ligand evolved to the enol form (Scheme 2)], although these changes are within the esds values.

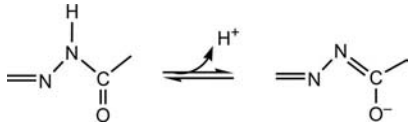

Scheme 2. Deprotonation of the SC chain and tautomeric evolution.

The hydrogen bonds in the two complexes of H_2L^3 are listed in Tables 9 and 10 and are represented in Figures S7 and S8. In $[PbPh_2(H_{0.5}L^3)(MeOH)](OAc)_{0.5}$ these interactions involve all of the N–H groups and the O atoms from the acetate group and the methanol molecule. It is worth noting the presence of the N(2)–H(2)···O(2) bond, which links the partially deprotonated hydrazinic group of the SC chain to the AcO^- anion. This hydrogen bond is the strongest of all the N–H···O bonds according to the bond lengths, and it fixes the H(2) atom well enough to be located in the difference maps – even though its occupation factor is only 0.5. It is tempting to hypothesize that this hydrogen bond provides us with a glimpse of the proton transfer from the donor [N(2)–H] to the acceptor (AcO^-) when the process is "under way".

Table 9. Hydrogen-bond lengths [Å] and angles [°] in $[PbPh_2(H_{0.5}L^3)(MeOH)](OAc)_{0.5}$.

D–H···A[a]	*d*(D–H)	*d*(H···A)	*d*(D···A)	<(DHA)
N(1)–H(1)···O(2)	0.86	2.56	3.276(6)	141.3
N(1)–H(1)···O(21)	0.86	2.15	2.985(7)	163.3
O(1s)–H(1s)···O(2)^{i}	0.56(5)	2.09(5)	2.613(6)	158(9)
O(1s)–H(1s)···O(21)^{ii}	0.56(5)	2.56(6)	2.897(7)	122(8)
N(2)–H(2)···O(2)	0.68(10)	2.17(10)	2.821(7)	159(12)
N(6)–H(6)···S^{iii}	0.86	2.77	3.370(4)	128.3

[a] Symmetry operators: i = $x - 1/2$, $y - 1/2$, z; ii = $-x + 1/2$, $y - 1/2$, $-z + 1/2$; iii = $-x$, $-y$, $-z + 1$.

Table 10. Hydrogen-bond lengths [Å] and angles [°] in $[PbPh_2(L^3)(dmso)]\cdot 2dmso$.

D–H···A[a]	*d*(D–H)	*d*(H···A)	*d*(D···A)	<(DHA)
N(1)–H(1)···O(2s1)	0.86	2.015	2.865(13)	169.6
N(6)–H(6)···O(3s)^{i}	0.86	2.080	2.925(12)	167.0

[a] Symmetry operators: i = x, $y + 1$, z.

In $[PbPh_2(L^3)(dmso)]\cdot 2dmso$, two N–H···O interactions link the uncoordinated dmso molecules to the complex (Figure S8).

^{1}H and ^{13}C NMR Spectroscopy

The ^{1}H and ^{13}C NMR spectroscopic data for SC^x and H_2L^x (see Scheme 1 for numbering) are listed in the Experimental Section. The assignment of the signals was initially based on those of related semicarbazones and thiosemicarbazones[8,16,17] and then confirmed by HMBC and HMQC experiments.

In the ^{1}H NMR spectra of SC^x, the integration of the signals associated with the N(2)H and N(1)H_2 [or N(1)HPh] groups indicates the presence of only one semicarbazone chain for each molecule (Scheme 3). The signal at δ = 197–199 ppm in the ^{13}C NMR spectra confirms that one of the carbonyl groups from the starting diketone remains unchanged.

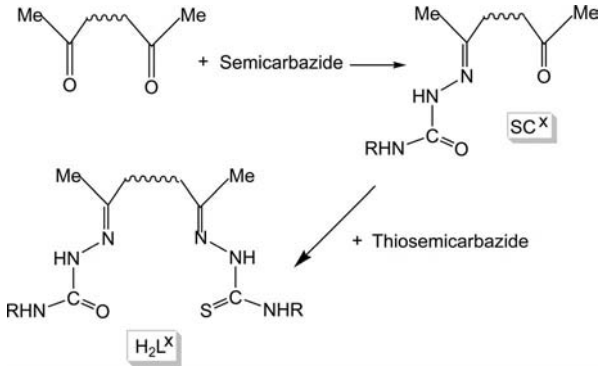

Scheme 3. Synthesis of semicarbazone/thiosemicarbazone ligands.

Condensation of the SC^x derivatives with the thiosemicarbazides and the formation of H_2L^x led to the appearance of additional signals in the ^{1}H NMR spectra, and these correspond to the NH and NH_2 (or NHR) groups of the new TSC chains. Furthermore, in the ^{13}C NMR spectra, the signal due to the remaining diketone carbonyl group vanished, and the appearance of two new signals at δ = 148 (C=N group) and 178 (C=S group) ppm confirmed the condensation of the thiosemicarbazide molecule.

The ^{1}H NMR spectrum of H_2L^1 in dmso shows some concentration-independent evolution of this compound (Figure 7). In a freshly prepared sample [spectrum (a)], the N(6)H proton from the TSC chain is highly deshielded (δ = 14.17 ppm), and only one set of signals is observed for each proton in the molecule. After 1 h [spectrum (b)], in addition to the signals in spectrum (a), a new set of signals appears, suggesting the presence of two different forms of the ligand in solution. After 24 h [spectrum (c)], only the signals corresponding to the second set remain, with the signal of the N(6)H proton at δ = 10.51 ppm. The spectrum of the freshly prepared sample probably corresponds to the ligand conformation found in the solid state, which has the strong N(6)–H···N(4) intramolecular hydrogen bond mentioned above (see discussion on X-ray data). This bond is probably responsible for the strong deshielding of the N(6)H proton[18] and also influences the mutual positions of the doublets associated with the pyridine C(4)H and C(6)H protons, which are 0.75 ppm apart in spectrum (a). The interaction with the solvent seemingly induces the evolution of the ligand to a second form [responsible for spectrum (c), Figure 7] in which the N(6)–H···N(4) bond is weakened or even disappears, thus increasing the shielding of the N(6)H proton and bringing the C(4)H and C(6)H doublets in the spectrum closer together. In this second form the TSC arm may adopt an "open" orientation[10] similar to that shown by the SC arm in the solid-state structure. This conformation with both arms in the "open-orientation" has been described for other related molecules.[19,20]

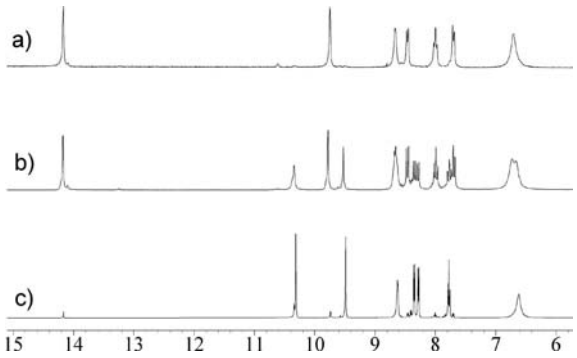

Figure 7. Evolution over time of the ^{1}H NMR spectrum of H_2L^1 in dmso solution: (a) t = 0, (b) t = 1 h, (c) t = 24 h. See the Experimental Section.

In the ^{1}H NMR spectrum of $[PbPh_2(HL^1)](OAc)_{0.75}Cl_{0.25}\cdot 2.375H_2O$, the presence of a very broad signal at δ = 11.82 ppm indicates that the N(2)H group remains intact. The integration of the acetate group for fewer than three protons is consistent with the presence of the chloride anion. Although there is no signal at low field that is directly attributable to N(2)H in the ^{1}H NMR spectrum of $[PbPh_2(OAc)(HL^2)]\cdot MeOH$, the presence of a very broad signal for HDO suggests that this proton possibly exchanges with water in the solvent.

The ^{1}H NMR spectra of the H_2L^3 complexes also reflect the protonation status of the ligand and are consistent with the solid-state study. Thus, in the spectrum of $[PbPh_2(L^3)(dmso)]\cdot 2dmso$, signals are not observed for N(2)H and N(6)H groups, as expected if the ligand is fully deprotonated. In the spectrum of $[PbPh_2(H_{0.5}L^3)(MeOH)](OAc)_{0.5}$, however, there is a broad signal at δ = 11.94 ppm and another narrow one at δ = 1.90 ppm, which integrate to 0.5 and 1.5 protons per mol of complex, respectively. Once again this is consistent with the previous formula in which half of the N(2)–H groups remain protonated, and there is 0.5 mol of acetate. Although this is the most obvious explanation for the NMR spectroscopic data, it is worth noting that another plausible interpretation for the results exists that is also coherent with the half-protonation of the SC chain in solid $[PbPh_2(H_{0.5}L^3)(MeOH)](OAc)_{0.5}$. The positions of the signals at δ = 11.94 and 1.90 ppm are rather similar to those observed for acetic acid in dmso solution (δ = 11.91 and 1.91 ppm[21]). Thus, under the influence of the solvent, the evolution to the fully deprotonated $(L^3)^{2-}$ ligand and HOAc cannot be ruled out. This alternative interpretation is supported by the isolation of only

$[PbPh_2(L^3)(dmso)]\cdot 2dmso$ when a dmso solution of $[PbPh_2(H_{0.5}L^3)(MeOH)](OAc)_{0.5}$ is concentrated to dryness (see the Experimental Section).

The values of $^3J(^1H\text{-}^{207}Pb)$ coupling constants in these compounds range from 208.6 to 226 Hz, that is, the expected values for a lead coordination number of six or above.[10,22] This suggests that the metal–ligand interactions described in the solid state probably remain in dmso solution.

Conclusion

We have described the synthesis of new H_2L^x multidentate ligands containing both SC and TSC arms and their complexation behaviour towards the $PbPh_2^{2+}$ ion in a methanol solution. All of the ligands readily form complexes with the organometallic cation, and these are stable at room temperature in air. The pentadentate character of the $(HL^1)^-$ anion derived from 2,6-diacetylpyridine permitted the isolation of a homoleptic complex, $[PbPh_2(HL^1)](OAc)_{0.75}Cl_{0.25}\cdot 2.375H_2O$. In this compound the donor atoms of the anion occupy all the equatorial positions of a pentagonal-bipyramidal coordination sphere in which the phenyl groups are in the apical positions. The H_2L^2 and H_2L^3 ligands derived from 2,3-butadione coordinate through only four donor atoms. This situation allows an additional donor atom from an acetate group or a molecule of solvent to enter the equatorial coordination plane, and this gives rise to heteroleptic complexes such as $[PbPh_2(OAc)(HL^2)]\cdot MeOH$.

In all the complexes, the TSC chain deprotonates easily, but the SC chain is clearly less acidic and remains protonated in the complexes of H_2L^1 and H_2L^2. The direct reaction of diphenyllead(IV) diacetate with H_2L^3 afforded a solid with the stoichiometry $[PbPh_2(H_{0.5}L^3)(MeOH)](OAc)_{0.5}$ in which, besides TSC deprotonation, an unusual partial deprotonation of the SC occurs with only half of the ligand molecules SC-deprotonated. When this complex was dissolved in dmso, the medium facilitated complete proton transfer, and the heteroleptic $[PbPh_2(L^3)(dmso)]\cdot 2dmso$ complex was formed.

Experimental Section

Reagents and Instruments: Commercially available chemicals, 2,6-diacetylpyridine (Aldrich), 2,3-butanedione (Aldrich), semicarbazide hydrochloride (Alfa), 4-phenyl-3-semicarbazide (Alfa), 4-methyl-3-thiosemicarbazide (Aldrich), 4-phenyl-3-thiosemicarbazide (Aldrich), diphenyllead(IV) dichloride (ABCR) and silver(I) acetate (Fluka) were reagent grade and were used as received. Diphenyllead(IV) diacetate was prepared[10] by the reaction of diphenyllead(IV) dichloride with silver(I) acetate in a 1:2 molar ratio in methanol. The silver(I) chloride formed was filtered off, and the solution containing the diphenyllead(IV) diacetate was used immediately in the preparation of the complexes. Elemental analyses for C, H, N and S were performed with a Fisons 1108 microanalyzer. Melting points were determined with an electrically heated Gallenkamp apparatus. IR spectra were recorded from KBr discs with a Bruker IFS66V FT-IR spectrophotometer and are reported in cm^{-1}. FAB^+ mass spectra were recorded with a VG AUTOSPEC spectrometer equipped with an OPUS system by using *m*-nitrobenzyl alcohol as matrix. NMR spectra were recorded in $[D_6]$-dmso with a Bruker AMX 300 spectrometer at 300.14 MHz for ^1H NMR spectra and at 75.4 MHz for ^{13}C NMR spectra (referenced to TMS by using the solvent signal; ^1H: δ = 2.50 ppm, ^{13}C: δ = 39.50 ppm). Elemental analysis and spectroscopic measurements were carried out by the RIAIDT services of the University of Santiago de Compostela.

Synthesis

Ligands: The synthesis of the asymmetric semicarbazone–thiosemicarbazone ligands was carried out according to a previously described procedure.[8] Briefly, the corresponding diketone was condensed with the semicarbazide hydrochloride in a 1:1 molar ratio, and the resulting monosemicarbazone (SC^x) was then condensed with the thiosemicarbazide in the same molar ratio (see Scheme 3).

H_2L^1: 2,6-Diacetylpyridine (1.60 g, 9.8 mmol) and distilled water (150 mL) were mixed in a 250 mL round-bottomed flask. A solution of semicarbazide hydrochloride (1.09 g, 9.8 mmol) in distilled water (30 mL) was slowly added to the suspension. The mixture was stirred and heated under reflux for 30 min, and the resulting cream coloured solid was isolated and characterized. Yield 84%; m.p. 219 °C. $C_{10}H_{12}N_4O_2$ (SC^1, diacetylpyridine semicarbazone) (220.23): calcd. C 54.54, H 5.49, N 25.44; found C 54.49, H 5.50, N 25.37. IR (KBr): $\tilde{\nu}$ = 3494 (m), 3361 (m), 3208 (m, N–H), 1730 (s), 1704 (s, C=O), 1575 (s, C=N), 1435 (s, ring) cm^{-1}. ^1H NMR ($[D_6]$dmso): δ = 9.89 [s, 1 H, N(2)H], 8.58 [d, 1 H, C(4)H], 7.94 [t, 1 H, C(5)H], 7.86 [d, 1 H, C(6)H], 6.69 [s, 2 H, $N(1)H_2$], 2.66, 2.33 [s, 6 H, $C(9,10)H_3$] ppm. ^{13}C NMR ($[D_6]$dmso): δ = 199.4 (C8), 156.9 (C2), 154.9 (C7), 151.8 (C3), 144.0 (C2), 137.5 (C5), 124.0 (C6), 120.5 (C4), 11.3, 25.4 (C9,C10) ppm. SC^1 (0.50 g, 2.27 mmol) and ethanol (50 mL) were mixed in a 250 mL round-bottomed flask. The suspension was heated and then mixed with a solution of 4-methyl-3-thiosemicarbazide (0.24 g, 2.27 mmol) in ethanol (55 mL). The pale yellow solution was heated under reflux for 4 h and stirred overnight. The resulting yellow precipitate was filtered off and characterized as H_2L^1. Yield 80%; m.p. 247–248 °C. $C_{12}H_{17}N_7OS$ (H_2L^1) (307.39): calcd. C 46.89, H 5.57, N 31.90, S 10.43; found C 46.80, H 5.67, N 31.76, S 10.50. FAB^+: *m*/*z* = 308 $[H_2L^1 + H]^+$, 293 $[H_2L^1 - Me + H]^+$. IR (KBr): $\tilde{\nu}$ = 3430 (m), 3363 (m) and 3110 (m, N–H), 1680 (s, C=O), 1579 (s), 1548 (s, C=N), 1433 (s, ring), 849 (m), 819 (m, C=S) cm^{-1}. ^1H NMR ($[D_6]$dmso); spectrum (a) (Figure 7): δ = 14.17 [s, 1 H, N(6)H], 9.76 [s, 1 H, N(2)H], 8.68 [q, 1 H, N(7)H], 8.46 [d, 1 H, C(6)H], 8.00 [t, 1 H, C(5)H], 7.70 [d, 1 H, C(4)H], 6.71 [s, 2 H $N(1)H_2$], 3.38, 2.37 [s, 6 H, $C(9,10)H_3$], 3.01 [d, 3 H, $C(12)H_3$] ppm. ^1H NMR ($[D_6]$dmso); spectrum (c) (Figure 7): δ = 10.31 [s, 1 H, N(6)H], 9.49 [s, 1 H N(2)H], 8.63 [q, 1 H, N(7)H], 8.35 [d, 1 H, C(6)H], 8.28 [d, 1 H, C(4)H], 7.72 [t, 1 H, C(5)H], 6.62 [s, 2 H, $N(1)H_2$], 3.05 [d, 3 H, $C(12)H_3$], 2.42, 2.31 [s, 6 H, $C(9,10)H_3$] ppm. ^{13}C NMR ($[D_6]$dmso); spectrum (c) (Figure 7): δ = 178.5 (C11), 156.8 (C1), 154.1 (C7), 153.3 (C3), 147.8 (C8), 144.5 (C2), 136.4 (C5), 120.0 (C4), 119.9 (C6), 31.1 (C12), 11.9 (C10), 11.3 (C9) ppm. Crystals suitable for X-ray analysis were grown from a solution of H_2L^1 in dmso at room temperature.

H_2L^2: 2,3-Butanedione (0.5 mL, 5.69 mmol) in water (10 mL) was added to semicarbazide hydrochloride (0.635 g, 5.69 mmol) in water (12 mL). The mixture was stirred for 30 min, and the resulting white solid was filtered off and identified. Yield 86%; m.p. 226 °C. $C_5H_9N_3O_2$ (SC^2, butanedione semicarbazone) (143.15): calcd. C 41.95, H 6.35, N 29.35; found C 41.89, H 6.38, N 29.09.

FAB$^+$: m/z = 144 [SC^2 + H]$^+$. IR (KBr): $\tilde{\nu}$ = 3493 (s), 3352 (s), 3106 (m, N–H), 1686 (s), 1603 (s, C=O), 1579 (s, C=N) cm^{-1}. ^{1}H NMR ([D$_6$]dmso): δ = 9.85 [s, 1 H, N(2)H], 6.71 [s, 2 H, N(1)H$_2$], 2.33, 1.84 [s, 6 H, C(3,5)H$_3$] ppm. ^{13}C NMR ([D$_6$]dmso): δ = 197.2 (C4), 156.2 (C1), 143.9 (C2), 24.39 (C5), 9.40 (C3) ppm. A solution of 4-methyl-3-thiosemicarbazide (0.36 g, 3.42 mmol) in ethanol (55 mL) was added to a suspension of SC^2 (0.49 g, 3.42 mmol) in ethanol (50 mL) along with a few drops of acetic acid. The suspension was heated under reflux for 4 h and stirred overnight. The small amount of white solid in suspension was removed by filtration and discarded. The clear solution was then stored for 24 h to afford a new white precipitate, which was filtered off and characterized as H_2L^2. Yield 33%; m.p. 252 °C. $C_7H_{14}N_6OS$ (H_2L^2) (230.29): calcd. C 36.51, H 6.13, N 36.49, S 13.90; found C 36.38, H 6.28, N 36.78, S 13.70. FAB$^+$: m/z = 231 [H_2L^2 + H]$^+$. IR (KBr): $\tilde{\nu}$ = 3468 (m) 3346 (m), 3265 (m), 3202 (m, N–H), 1683 (s, C=O), 1594 (m), 1554 (s, C=N), 955 (w, C=S) cm^{-1}. ^{1}H NMR ([D$_6$]dmso): δ = 10.09 [s, 1 H, N(5)H], 9.37 [s, 1 H, N(2)H], 8.27 [q, 1 H, N(6)H], 6.45 [s, 2 H, N(1)H$_2$], 2.99 [d, 3 H, C(7)H$_3$], 2.06, 2.12 [s, 6 H, C(3,5)H$_3$] ppm. ^{13}C NMR ([D$_6$]dmso): δ = 178.4 (C6), 156.5 (C1), 148.4 (C4), 144.9 (C2), 31.1 (C7), 11.4 (C5), 11.0 (C3) ppm.

H_2L^3: 4-Phenyl-3-semicarbazide (0.86 g, 5.69 mmol) in water (70 mL) was added to an aqueous solution of 2,3-butanedione (0.50 mL, 5.69 mmol) in water (10 mL). The mixture was stirred for 1.5 h, and the resulting solid was isolated. Yield 84%; m.p. 229–230 °C. $C_{11}H_{13}N_3O_2$, (SC^3, butanedione phenylsemicarbazone) (219.10): calcd. C 60.25, H 5.98, N 19.17; found C 60.01, H 6.09, N 19.38. FAB$^+$: m/z = 220 [SC^3 + H]$^+$. IR (KBr): $\tilde{\nu}$ = 3379 (m), 3367 (m), 3199 (m, NH), 1698 (s), 1686 (s, C=O), 1595 (s, C=N) cm^{-1}. ^{1}H NMR ([D$_6$]dmso): δ = 10.25 [s, 1 H, N(2)H], 8.96 [s, 1 H, N(1)H], 7.57 (d, 2 H, H$_o$-Ph), 7.31 (t, 2 H, H$_m$-Ph), 7.04 (t, 1 H, H$_p$-Ph), 1.91, 2.44 [s, 6 H, C(3,5)H$_3$] ppm. ^{13}C NMR ([D$_6$]dmso): δ = 197.2 (C4), 154.3 (C2), 152.4 (C1), 138.5 (C$_i$), 128.6 (C$_m$), 123.0 (C$_p$), 120.0 (C$_o$), 24.6 (C5), 9.6 (C3) ppm. SC^3 (0.24 g, 1.10 mmol), 4-phenyl-3-thiosemicarbazide (0.17 g, 1.12 mmol) and ethanol (25 mL) were introduced into a 50 mL flask. The yellow suspension was stirred for 17 h and then filtered. This first solid isolated was identified as a small amount of SC^3. The mother liquor, when slowly concentrated at room temperature for 24 h, afforded H_2L^3. Yield 30%; m.p. 239 °C. $C_{18}H_{20}N_6OS$ (H_2L^3) (368.46): calcd. C 58.68, H 5.47, N 22.81, S 8.70; found C 58.50, H 5.35, N 22.58, S 8.51. FAB$^+$: m/z = 369 [H_2L^3 + H]$^+$. IR (KBr): $\tilde{\nu}$ = 3373 (w), 3312 (w), 3188 (w, N–H), 1681 (s, C=O), 1595 (m), 1546 (s, C=N), 1032 (w, C=S) cm^{-1}. ^{1}H NMR ([D$_6$]dmso): δ = 10.58 [s, 1 H, N(5)H], 9.92 [s, 1 H, N(2)H], 9.92 [s, 1 H, N(6)H], 8.79 [s, 1 H, N(1)H], 7.58 (d), 7.29 (t), 7.02 (t, 5 H, Ph(SC)], 7.58 (d), 7.36 (t), 7.20 (t, 5 H Ph(TSC)], 2.30, 2.20 [s, 6 H, C(3,5)H$_3$] ppm. ^{13}C NMR ([D$_6$]-dmso): δ = 176.8 (C6), 152.9 (C1), 149.4 (C4), 146.5 (C2), 139.0, 128.1, 125.5, 125.4 [Ph(TSC)], 138.7, 128.5, 122.6, 119.7 [Ph(SC)], 12.0 (C5), 11.5 (C3) ppm.

Complexes: Diphenyllead(IV) complexes of the semicarbazone/thiosemicarbazone ligands H_2L^1–H_2L^3 were obtained by treating the corresponding ligand with a freshly prepared methanolic solution of diphenyllead(IV) diacetate in a 1:1 molar ratio.

Caution! Lead is a highly toxic cumulative poison. Lead compounds should be handled carefully.[5]

[PbPh$_2$(HL^1)](OAc)$_{0.75}$Cl$_{0.25}$·2.375H$_2$O: A recently prepared solution of diphenyllead(IV) diacetate (0.15 g, 0.31 mmol) in methanol (25 mL) was added to a suspension of H_2L^1 (0.10 g, 0.32 mmol) in methanol (30 mL). The resulting solution was stirred for 20 h and then stored at room temperature for a few days. A small amount of yellow crystalline solid had formed and was filtered off. Yield 20% (first batch); m.p. 198 °C. $C_{25.5}H_{33}Cl_{0.25}N_7O_{4.88}SPb$ {[PbPh$_2$(HL^1)](OAc)$_{0.75}$Cl$_{0.25}$·2.375H$_2$O} (763.79): calcd. C 40.10, H 4.35, N 12.84, S 4.20; found C 39.85, H 4.20, N 12.38, S 3.98. FAB$^+$: m/z = 668 [(PbPh$_2$)(HL^1)]$^+$, 590 [(PbPh)(HL^1)]$^+$, 307 [HL^1 + H]$^+$. IR (KBr): $\tilde{\nu}$ = 3375 (m), 3051 (m, N–H), 1671 (m, C=O), 1566 (m), 1433 m (m, OAc, $\Delta\tilde{\nu}$ = 133), 1503 (m), 1474 (m, C=N), 1382 (s, ring), 805 (w, C=S) cm^{-1}. ^{1}H NMR ([D$_6$]dmso): δ = 11.82 [br. s, 1 H, N(2)H], 8.06 [t, 1 H, C(5)H], 7.72 [d, 1 H, C(6)H], 7.70 [d, 1 H C(4)H], 7.46 [d, ^3J(^{1}H-^{207}Pb) = 226 Hz, 4 H, H$_o$-(PbPh)], 7.28 [t, 4 H, H$_m$-(PbPh)], 7.19 [t, 2 H, H$_p$-(PbPh)], 7.15 [br. s, 1 H, N(7)H], 6.45 [br. s, 2 H, N(1)H$_2$], 2.91 [d, 3 H, C(12)H$_3$], 2.57, 2.38 [s, 6 H, C(9,10)H$_3$], 1.90 (s, 2.25 H, $^-$OAc) ppm. Crystals of [PbPh$_2$(HL^1)](OAc)$_{0.75}$Cl$_{0.25}$·2.375H$_2$O suitable for X-ray studies were obtained from the mother liquors.

[PbPh$_2$(OAc)(HL^2)]·MeOH: A freshly prepared methanolic solution of diphenyllead(IV) diacetate (0.208 g, 0.43 mmol in 25 mL) was added to a suspension of H_2L^2 (0.10 g, 0.43 mmol) in methanol (30 mL). The resulting yellow solution was stirred and heated under reflux for 7 h and then concentrated under vacuum until a fine grey suspension appeared. This solid was removed by filtration, and the clear solution was slowly concentrated at room temperature for a few days until a precipitate formed. This solid comprised two types of crystals; white needles of diphenyllead(IV) diacetate and yellow prisms of the title complex; m.p. 201 °C. $C_{22}H_{30}N_6O_4PbS$ {[PbPh$_2$(OAc)(HL^2)]·MeOH} (681.77): calcd. C 38.76, H 4.44, N 12.33, S 4.47; found C 38.48, H 4.60, N 12.55, S 4.67. FAB$^+$: m/z = 591 [PbPh$_2$(HL^2)]$^+$, 437 [Pb(HL^2)]$^+$. IR (KBr): $\tilde{\nu}$ = 3332 (m), 3127 (m), 3051 (m, N–H), 1675 (s, C=O), 1565 (s), 1334 (s, OAc, $\Delta\tilde{\nu}$ = 231), 1553 (s), 1529 (s, C=N), 734 (m, C=S) cm^{-1}. ^{1}H NMR ([D$_6$]dmso): δ = 7.83 [d, ^3J(^{1}H-^{207}Pb) = 208.6 Hz, 4 H, H$_o$-(PbPh)], 7.40 [t, 4 H, H$_m$-(PbPh)], 7.29 [t, 2 H, H$_p$-(PbPh)], 6.94 [br. s, 1 H, N(6)H], 6.03 [s, 2 H, N(1)H$_2$], 4.11 [m, 1 H, OH(MeOH)], 3.16 [d, 3 H, CH$_3$(MeOH)], 2.77 [d, 3 H, C(7)H$_3$], 2.28, 2.14 [s, 6 H, C(3,5)H$_3$], 1.83 (s, 3 H, $^-$OAc) ppm. A very broad signal is observed for HDO.

[PbPh$_2$(H$_{0.5}$L^3)(MeOH)](OAc)$_{0.5}$: A solution of diphenyllead(IV) diacetate (0.13 g, 0.27 mmol) in methanol (25 mL) was slowly added to a suspension of H_2L^3 (0.10 g, 27.1 mmol) in methanol (22 mL). The resulting orange mixture was heated under reflux and stirred for 5 h. The mixture was cooled to room temperature, and a small amount of a dark solid was filtered off and discarded. The mother liquor afforded an orange crystalline solid after 2 d of slow concentration. Yield 50%; m.p. 189 °C. $C_{32}H_{34}N_6O_3PbS$, {[PbPh$_2$(H$_{0.5}$L^3)(MeOH)](OAc)$_{0.5}$} (789.91): calcd. C 48.66, H 4.34, N 10.64, S 4.06; found C 48.52, H 4.20, N 10.66, S 3.95. FAB$^+$: m/z = 729 [PbPh$_2$(HL^3)]$^+$. IR (KBr): $\tilde{\nu}$ = 3197 (w), 3052 (w), 2987 (w, N–H), 1667 (m, C=O), 1602 (s), 1313 (s, OAc, $\Delta\tilde{\nu}$ = 289), 1518 (s), 1493 (s, C=N), 692 (m, C=S) cm^{-1}. ^{1}H NMR ([D$_6$]-dmso): δ = 11.92 [br. s, 0.5 H, N(2)H], 9.16 [s, 1 H, N(6)H], 9.01 [s, 1 H, N(1)H], 7.90 [d, ^3J(^{1}H-^{207}Pb) = 210.1 Hz, 4 H, H$_o$-(PbPh)], 7.70, 7.63 (d, 4 H, H$_o$), 7.43 [t, 4 H, H$_m$-(PbPh)], 7.30, 7.19 (m, 4 H, H$_m$), 7.23 [t, 2 H, H$_p$-(PbPh)], 6.89, 6.83 (t, 2 H, H$_p$), 4.09 [q, 1 H, OH(MeOH)], 3.17 [d, 3 H, CH$_3$(MeOH)], 2.30, 2.38 [s, 6 H, C(3,5)H$_3$], 1.91 (s, 1.5 H, $^-$OAc) ppm. The same results were obtained when the reaction mixture was refluxed and stirred for 2 d. From the crystalline orange solid, a single crystal of composition [PbPh$_2$(H$_{0.5}$L^3)(MeOH)](OAc)$_{0.5}$ was selected and studied by X-ray diffraction. A portion of this solid was recrystallised from dmso to afford single crystals of composition **[PbPh$_2$(L^3)(dmso)]·2dmso**: $C_{36}H_{46}N_6O_4PbS_4$ (962.24): calcd. C 44.94, H 4.82, N 8.73, S 13.32; found C 44.89, H 4.61, N 8.75, S 13.01. ^{1}H NMR ([D$_6$]dmso): δ = 9.15 [s, 1 H, N(6)H], 9.01 [s, 1 H, N(1)H], 7.91 [d, ^3J(^{1}H-^{207}Pb) = 208.0 Hz, 4 H, H$_o$-(PbPh)], 7.70, 7.63 (d, 4 H, H$_o$), 7.43 [t, 4 H,

Table 11. Crystal data, data collection and refinement for the ligand and complexes.

	H_2L^1	$[PbPh_2(HL^1)](OAc)_{0.75}Cl_{0.25}\cdot 2.375H_2O$	$[PbPh_2(OAc)(HL^2)]\cdot MeOH$	$[PbPh_2(H_{0.5}L^3)(MeOH)](AcO)_{0.5}$	$[PbPh_2(L^3)(dmso)]\cdot 2dmso$
Empirical formula	$C_{12}H_{17}N_7OS$	$C_{25.5}H_{33}Cl_{0.25}N_7O_{4.88}PbS$	$C_{22}H_{30}N_6O_4PbS$	$C_{64}H_{68}N_{12}O_6Pb_2S_2$	$C_{36}H_{46}N_6O_4PbS_4$
Formula mass	307.39	763.7	681.77	1579.80	962.22
T [K]	100.0(1)	100.0(1)	110.0(2)	100.0(1)	110.0(2)
Crystal system	monoclinic	monoclinic	monoclinic	monoclinic	triclinic
Space group	$P2_1/n$	$C2/c$	$P2_1/n$	$C2/c$	$P\bar{1}$
a [Å]	8.2319(3)	23.0384(17)	9.9325(7)	13.0041(8)	9.6563(3)
b [Å]	20.5305(7) A	16.6605(13)	15.1109(10)	13.8846(8)	14.4927(5)
c [Å]	9.1091(4)	17.1170(14)	17.3815(13)	33.6220(19)	15.4194(5)
α [°]	90	90	90	90	100.312(2)
β [°]	113.414(2)	105.479(4)	103.313(4)	91.169(3)	95.718(2)
γ [°]	90	90	90	90	108.599(2)
V [Å^3]	1412.72(9)	6331.7(9)	2538.7(3)	6069.4(6)	1983.52(11)
Z	4	8	4	4	2
μ [mm]$^{-1}$	0.241	5.460	6.768	5.673	4.509
Crystal size [mm]	$0.24\times0.11\times0.03$	$0.20\times0.10\times0.09$	$0.21\times0.10\times0.09$	$0.60\times0.13\times0.11$	$0.15\times0.08\times0.02$
θ range [°]	2.63–26.44	2.44–26.02	1.81–26.39	2.15–26.02	1.52–22.87
Reflections collected	9643	29477	21023	40538	77234
Unique data	2996	6212	5196	5946	5299
R_{int}	0.0399	0.0350	0.0564	0.0554	0.0506
GOF	1.030	1.075	1.007	1.053	1.074
R_1 [$I>2\sigma(I)$]	0.0470	0.0362	0.0361	0.0285	0.0500
(all data)	0.0732	0.0641	0.0726	0.0398	0.0580
wR_2 [$I>2\sigma(I)$]	0.1000	0.0873	0.0608	0.0533	0.1176
(all data)	0.1105	0.1010	0.0722	0.0558	0.1255
Residual electron density [e Å^{-3}]	0.847/–0.410	1.463/–1.804	2.043/–1.525	1.903/–0.796	3.153/–2.287

H_m-(PbPh)], 7.30, 7.19 (t, 4 H, H_m), 7.25 [t, 2 H, H_p-(PbPh)], 6.89, 6.83 (t, 2 H, H_p), 2.54 [s, 18 H, CH_3(dmso)], 2.39, 2.30 [s, 6 H, C(3,5)H_3] ppm. Removal of the solvent to dryness, after a few weeks of slow concentration, showed the complete evolution of $[PbPh_2(H_{0.5}L^3)(MeOH)](OAc)_{0.5}$ to $[PbPh_2(L^3)(dmso)]\cdot 2dmso$.

X-ray Crystallography: Crystal data were collected at low temperature with a Bruker Kappa-APEX II diffractometer using Mo-K_α radiation (RIAIDT, University of Santiago de Compostela). Data were corrected for absorption by multi-scans (SADABS).[23] Structures were solved by direct methods in the case of the ligand H_2L^1 and the Patterson method for all the complexes, followed by normal difference Fourier techniques. The program used was SHELX97.[24] Although the diffraction data for $[PbPh_2(L^3)(dmso)]\cdot 2dmso$ were not of very good quality (probably due to the small size of the crystal), the successive refinements allowed atomic positions and structural information to be obtained with reasonable accuracy. Hydrogen atoms were included in idealized positions and refined by using a riding model, except those of H_2L^1 and H(2) and H(1s) of $[PbPh_2(H_{0.5}L^3)(MeOH)](OAc)_{0.5}$, which were located from the difference maps. Some disorder was found not only in the solvent molecules in $[PbPh_2(HL^1)](OAc)_{0.75}Cl_{0.25}\cdot 2.375H_2O$, but also in the acetate ligand in $[PbPh_2(OAc)(HL^2)]\cdot MeOH$ and in the dmso molecules in $[PbPh_2(L^3)(dmso)]\cdot 2dmso$. In the latter, this disorder affects the dmso molecules 1 and 2. In molecule 1, the anisotropic displacement parameters and the bond lengths were restrained to be similar by using SIMU. Molecule 2, in which the disorder mainly affects the oxygen atom, was modelled over two positions whose s.o.f. were 0.8 and 0.2. Atomic displacement parameters for all the atoms in this molecule, except S(2S), were constrained to be identical by using free variables. Molecular graphics were obtained with ORTEP[25] and MERCURY.[26] Crystal data, experimental details and refinement results are listed in Table 11. CCDC-794199 (for H_2L^1), -794200 {for $[PbPh_2(HL^1)](OAc)_{0.75}Cl_{0.25}\cdot 2.375H_2O$}, -794201 {for $[PbPh_2(OAc)(HL^2)]\cdot MeOH$}, –794202 {for $[PbPh_2(H_{0.5}L^3)(MeOH)](OAc)_{0.5}$} and -794203 {for $[PbPh_2(L^3)(dmso)]\cdot 2dmso$} contain the supplementary crystallographic data for this paper. These data can be obtained free of charge from The Cambridge Crystallographic Data Centre via www.ccdc.cam.ac.uk/data_request/cif.

Supporting Information (see footnote on the first page of this article): Figures S1–S3 and S5–S8 showing the hydrogen bonding interactions in the lattices of H_2L^1 and complexes; Figure S4 showing the packing of chains in the network of $[PbPh_2(HL^1)](OAc)_{0.75}Cl_{0.25}\cdot 2.375H_2O$.

Acknowledgments

We thank the Spanish Ministry of Education and Science (Project CTQ2006-11805) and the Spanish Ministry of Science and Innovation (Project CTQ2009-10738) for financial support.

[1] S. Bradberry, T. Sheehan, A. Vale, *QJM* **2009**, *102*, 721–732.
[2] P. A. Meyer, M. J. Brown, H. Falk, *Mutat. Res.* **2008**, *659*, 166–175.
[3] H. Gurer, N. Ercal, *Free Radical Biol. Med.* **2000**, *29*, 927–945.
[4] R. L. Davidovich, *Russ. J. Coord. Chem.* **2005**, *31*, 455–466.
[5] S. J. S. Flora, G. Flora, G. Saxena in *Lead Chemistry, Analytical Aspects, Environmental Impact and Health Effects* (Eds.: J. S. Casas, J. Sordo), Elsevier, Amsterdam, **2006**, p. 158.
[6] S. Bradberry, A. Vale, *Clin. Toxicol.* **2009**, *47*, 617–631.
[7] S. G. Schäfer, R. L. F. Dawes, B. Elenhans, W. Forth, K. Schümann in *Toxicolagy* (Eds.: H. Marquardt, S. G. Schäfer, R. O. McClellan, F. Welsch), Academic Press, San Diego, **1999**, p. 755.
[8] A. Jagst, A. Sánchez, E. M. Vázquez-López, U. Abram, *Inorg. Chem.* **2005**, *44*, 5738–5744.

[9] J. S. Casas, M. S. García-Tasende, J. Sordo, *Coord. Chem. Rev.* **2000**, *209*, 197–261.
[10] J. S. Casas, E. E. Castellano, J. Ellena, M. S. García-Tasende, F. Namor, A. Sánchez, J. Sordo, M. J. Vidarte, *Eur. J. Inorg. Chem.* **2007**, *27*, 3742–3750.
[11] R. Pedrido, A. M. González-Noya, M. J. Romero, M. Martínez-Calvo, M. Vázquez López, E. Gómez-Fórneas, G. Zaragoza, M. R. Bermejo, *Dalton Trans.* **2008**, *47*, 6776–6787.
[12] F. H. Allen, *Acta Crystallogr., Sect. B* **2002**, *58*, 380–388.
[13] J. S. Casas, M. V. Castaño, M. C. Cifuentes, J. C. García-Monteagudo, A. Sánchez, J. Sordo, A. Touceda, *J. Organomet. Chem.* **2007**, *692*, 2234–2244.
[14] J. S. Casas, E. E. Castellano, J. Ellena, M. S. García-Tasende, A. Sánchez, J. Sordo, A. Touceda, *Polyhedron* **2008**, *27*, 1–11.
[15] J. S. Casas, E. E. Castellano, J. Ellena, M. S. García-Tasende, A. Sánchez, J. Sordo, A. Touceda, *Polyhedron* **2009**, *28*, 1029–1039.
[16] J. S. Casas, A. Castiñeiras, A. Sánchez, J. Sordo, A. Vázquez-López, M. C. Rodríguez-Argüelles, U. Russo, *Inorg. Chim. Acta* **1994**, *221*, 61–68.
[17] K. Nomiya, K. Sekino, M. Ishikawa, A. Honda, M. Yokoyama, N. C. Kasuga, H. Yokoyama, S. Nakano, K. Onodera, *J. Inorg. Biochem.* **2004**, *98*, 601–615.
[18] C. A. Brown, D. X. West, *Transition Met. Chem.* **2003**, *28*, 154–159.
[19] M. Vázquez, L. Fabbrizzi, A. Taglietti, R. M. Pedrido, A. M. González-Noya, M. R. Bermejo, *Angew. Chem.* **2004**, *116*, 1996; *Angew. Chem. Int. Ed.* **2004**, *43*, 1962–1965.
[20] M. A. Ali, A. H. Mirza, W. B. Ejau, P. V. Bernhardt, *Polyhedron* **2006**, *25*, 3337–3342.
[21] R. J. Abraham, J. J. Byrne, L. Griffiths, M. Perez, *Magn. Reson. Chem.* **2006**, *44*, 491–509.
[22] S. N. Ólafsson, C. Flensburg, P. Andersen, *J. Chem. Soc., Dalton Trans.* **2000**, *23*, 4360–4368.
[23] *SADABS*, Bruker AXS Inc., Madison, Wisconsin, USA, **2001**.
[24] G. M. Sheldrick, *SHELX-97*, *An Integrated System for Solving and Refining Crystal Structures from Diffraction Data*, University of Göttingen, Göttingen, Germany, **1997**.
[25] *ORTEP III* for Windows: L. J. Farrugia, *J. Appl. Crystallogr.* **1997**, *30*, 565.
[26] *MERCURY*, New Software for Searching the Cambridge Structural Database and Visualising Crystal Structures: I. J. Bruno, J. C. Cole, P. R. Edgington, M. K. Kessler, C. F. Macrae, P. McCabe, J. Pearson, R. Taylor, *Acta Crystallogr., Sect. B* **2002**, *58*, 389–397.

Received: September 28, 2010
Published Online: January 13, 2011

